TRR
JOURNAL OF THE TRANSPORTATION RESEARCH BOARD

Research Article

Transportation Research Record
1–12

DOI: 10.1177/0361198120972714
journals.sagepub.com/home/trr
SAGE

Developing City-Wide Hurricane Impact Maps using Real-Life Data on Infrastructure, Vegetation and Weather

Mingyang Chen[1], Alican Karaer[1], Eren Erman Ozguven[1], Tarek Abichou[1], Reza Arghandeh[2], and Jaap Nienhius[3]

Abstract

Hurricanes affect thousands of people annually, with devastating consequences such as loss of life, vegetation and infrastructure. Vegetation losses such as downed trees and infrastructure disruptions such as toppled power lines often lead to roadway closures. These disruptions can be life threatening for the victims. Emergency officials, therefore, have been trying to find ways to alleviate such problems by identifying those locations that pose high risk in the aftermath of hurricanes. This paper proposes an integrated methodology that utilizes both Google Earth Engine (GEE) and geographical information systems (GIS). First, GEE is used to access Sentinel-2 satellite images and calculate the Normalized Difference Vegetation Index (NDVI) to investigate the vegetation change as a result of Hurricane Michael in the City of Tallahassee. Second, through the use of ArcGIS, data on wind speed, debris, roadway density and demographics are incorporated into the methodology in addition to the NDVI indices to assess the overall impact of the hurricane. As a result, city-wide hurricane impact maps are created using weighted indices created based on all these data sets. Findings indicate that the northeast side of the city was the worst affected because of the hurricane. This is a region where more seniors live, and such disruptions can lead to dramatic consequences because of the fragility of these seniors. Officials can pinpoint the identified critical locations for future improvements such as roadway geometry modification and landscaping justification.

Natural disasters such as hurricanes affect thousands of people annually with devastating consequences such as loss of life, vegetation and infrastructure. Unfortunately, the number of catastrophic hurricanes that have struck the U.S. Gulf States such as Florida has increased over recent years. National Oceanic and Atmospheric Administration (NOAA) data shows that the South Atlantic region suffered 15 named storms, eight hurricanes and two major hurricanes in 2018, considerably more than the annual average of 12.1 named storms, 6.4 hurricanes and 2.7 major hurricanes from 1981 to 2010 (*1*). Hurricane Michael, for example, was a highly destructive hurricane that struck the whole Florida Panhandle in 2018, and was the first Category 5 hurricane to strike the area since Hurricane Andrew in 1992. Michael made a landfall with peak winds of more than 150 mph (240 km/h) and affected the states of Florida, Georgia, North Carolina and even Virginia, causing directly or indirectly the deaths of 59 people. The total damage caused by Hurricane Michael was estimated to be approximately $25 billion by the NOAA National Centers for Environmental Information (*2*). As a result of the high winds, vegetation losses such as downed trees and infrastructure disruptions such as toppled power lines led to substantial roadway closures within the affected region. These roadway disruptions reduced the accessibility and increased the emergency response travel time, which created life threatening consequences for the victims. Emergency officials, since then, have been trying to find ways to alleviate roadway-related disruptions by assessing the current roadway conditions and identifying those locations that pose high risk in the aftermath of such a hurricane.

Multiple studies have spatially and statistically investigated the effect and damage of hurricanes. For example,

[1]Department of Civil & Environmental Engineering, FAMU & FSU College of Engineering, Tallahassee, FL
[2]Department of Computing, Mathematics, and Physics, Western Norway University of Applied Sciences, Bergen, Norway
[3]Department of Physical Geography, Utrecht University, Utrecht, The Netherlands

Corresponding Author:
Mingyang Chen, mc15an@my.fsu.edu

Ulak et al. (*3*) evaluated the hurricane-induced power outages because of Hurricane Hermine, and found that victims affected by outages were spatially clustered at particular regions rather than being distributed randomly. As such, vulnerable locations should be identified and effective strategies should be developed by cities and other relevant agencies to reduce such damage caused by hurricanes. Eskandarpour and Khodaei (*4*) performed a similar disaster risk assessment and developed a machine learning based method to predict potential outage of power grid components.There are also many approaches that have focused on the hurricane-induced high wind risk. For instance, Shao et al. (*5*) investigated historical hurricane data and pointed out that policies should pay more intention to wind risks and fully incorporate these risks into hazard reduction plans. A case study of Hurricane Isabel was carried out by Ning et al. (*6*) to study multiple hazards from hurricanes. Their findings indicated that wind damage was not necessarily restricted to the areas closest to the storm but also affected other areas substantially.

Roadway networks are known to be one of the infrastructure systems highly vulnerable to hurricanes. As such, numerous studies have focused on the accessibility, resilience, vulnerability and damage associated with roadway networks. Kocatepe et al. (*7*) proposed a new index, namely the Accessibility Decrease Index, to measure the emergency response travel time in the City of Tallahassee after Hurricane Hermine. Results showed those areas with less accessibility and roadways that had high risk of closure during the one-week period after Hermine hit the city. Chang (*8*) similarly assessed overall performances and distributional impacts based on the concept of accessibility. It was found that the distributions of loss and damage had spatial disparities, and alternative restoration priorities should be designed from a systems perspective. Li et al. (*9*), on the other hand, developed a scenario-based model to select shelter locations to optimize the evacuation needs under hurricane events. It was mentioned that different hurricane scenarios should be considered, and transportation demands should be collected when selecting locations for public shelters. Wilmot and Mei (*10*) evaluated a different trip generation model for hurricane evacuations and stated that the logistic regression and neural network models performed better than the participation rate model. Wolshon et al. (*11*) reviewed hurricane evacuation models and discussed policies and practices for transportation systems including planning, operation, management, and response. The study showed the need for better signs to provide better information for the public in the context of improving hurricane evacuations. The significant contribution was to forecast the evacuation travel demand and conduct an evacuation traffic analysis through the application of intelligent transportation systems (ITS) technologies based on the concept of convolutional neural network, a well-known machine learning technique. Recently, Ghorbanzadeh et al. (*12*) studied the power outages and roadway closures in the City of Tallahassee based on real-life data on the impacts of Hurricane Hermine (2016) and Michael (2018) throughout the city. The study showed those locations that were under high risk of electricity outages and roadway disruptions, both statistically and spatially.

With recent improvements in the technology, remote sensing and satellite image processing have been playing more important roles in hurricane-related studies. For example, Knorn et al. (*13*) adapted the support vector machines algorithm, whereas Shalaby and Tateishi (*14*) used a supervised classification methodology in the context of image processing. Both showed high accuracy of land use classification using data extracted from satellite images. Noi and Kappas (*15*) compared different classifiers for land cover classification using Sentinel-2 image data, and indicated that the classification resulted in high overall accuracy, ranging from 90% to 95%. Similarly, Aljoufie et al. (*16*) showed that remote sensing technology could be applicable for analyzing the spatiotemporal relationship between urban growth and transportation. They developed eight urban growth and transportation indices to extract information from satellite images.

Many studies also take advantage of geographical information systems (GIS)-based tools for remote sensing and satellite image processing purposes. Some of the recent remote sensing studies, on the other hand, have benefited from a newly-developing tool called Google Earth Engine (GEE), which greatly increases the accessibility of satellite data. For example, van Hell (*17*) analyzed hurricane-induced land cover change from Sentinel-2 optical images using GEE. The satellite image was conveniently retrieved from the Earth Engine server. Indices that highlight vegetation, sand and urban areas in the images were calculated. Classification and validation processes were performed online to show the change in each aspect. Johansen et al. (*18*) evaluated the clearing of woody vegetation in Australia through GEE. Four approaches were investigated to detect the changes using Landsat-5 TM and 7 ETM + time-series satellite images. Results showed that the Normalized Difference Vegetation Index (NDVI) was the most robust for calculating vegetation clearing probability.

A few studies have integrated GEE and GIS to focus on the impact of hurricanes (*19*, *20*). However, to the authors' knowledge, none of the existing studies have integrated them to focus on the impact of hurricanes based on real-life data. In this paper, GEE is used to access Sentinel-2 satellite images and NDVI indices calculated to investigate the vegetation change that

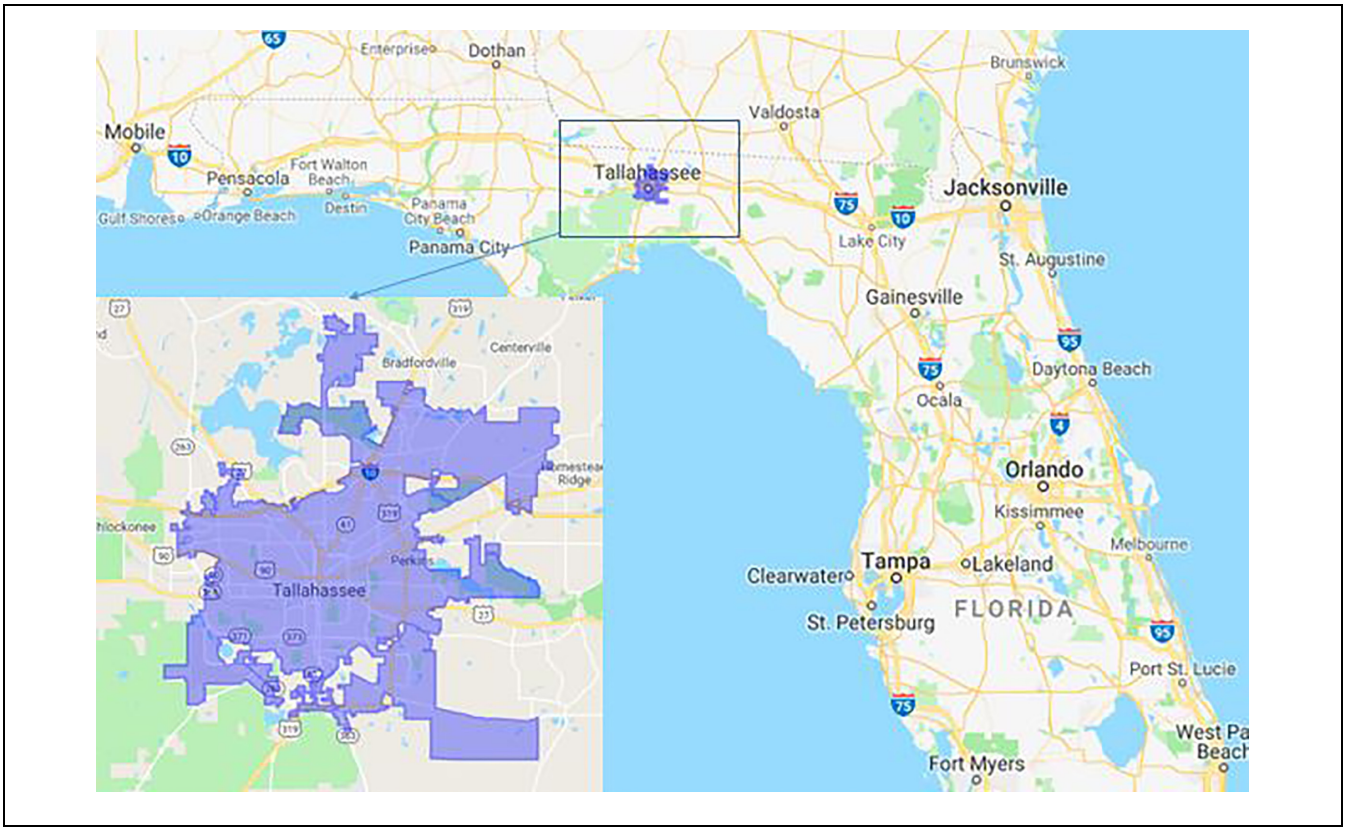

Figure 1. Map of part of Florida, showing the study area.

happened as a result of Hurricane Michael in the City of Tallahassee. Data on wind speed, debris, roadway density and demographics were also incorporated into the integrated methodology in addition to the NDVI indices to assess the impact of hurricane on the city. This type of analysis can be critical for analyzing the impact associated with roadway disruptions. As such, officials can use the findings of this research to pinpoint those locations that pose high risk and develop better plans and policies to improve the performance of the overall emergency transportation operations.

Methodology

Study Area, Hurricane Michael and Data

In this paper, a case study was created with a focus on the City of Tallahassee, the capital of Florida (Figure 1). Tallahassee had a population of 193,551 as of year 2018 and it can be considered as mid-size city. There are two major universities in Tallahassee, namely Florida State University (FSU) and Florida Agricultural and Mechanical University (FAMU). As a result, 35% of the entire population are students (*21*). In addition, since it is the state capital, Tallahassee is the site for the Florida State Capitol, Supreme Court of Florida, Florida Governor's Mansion, and nearly 30 state agency headquarters. As such, it is critical for the transportation network in the city to be operational even in the aftermath of hurricanes.

Hurricane Michael, a Category 5 hurricane, made landfall near Mexico Beach in the Florida Panhandle region on October 10, 2018. The storm led to maximum sustained wind speeds of 161 mph (259 km/h) and pushed a massive and destructive storm surge to the coast, which resulted in catastrophic damage, particularly in those areas closer to Panama City and Mexico Beach (*2*). Michael surfed over land and pushed strong winds and rain inland, and affected Tallahassee drastically although it did not pass through the city. Maximum wind speeds of 71 mph (114 km/h) were reached during Hurricane Michael in Tallahassee. As a result of these high winds, vegetation losses such as downed trees and infrastructure disruptions such as toppled power lines led to substantial roadway closures in the city. In several locations, power outages and roadway closures lasted approximately a week, and roadway closures made it very difficult for the public to commute and for emergency vehicles to respond to problems (*22*).

In this study, several datasets were used to conduct the proposed methodology. First of all, Sentinel-2 satellite imagery was used to calculate the vegetation change,

Table 1. Band Information of Sentinel-2 Satellite

Sentinel-2 bands	Central wavelength (μm)	Resolution (m)
Band 1—Coastal aerosol	0.443	60
Band 2—Blue	0.490	10
Band 3—Green	0.560	10
Band 4—Red	0.665	10
Band 5—Vegetation red edge	0.705	20
Band 6—Vegetation red edge	0.740	20
Band 7—Vegetation red edge	0.783	20
Band 8—Near infrared	0.842	10
Band 8A—Vegetation red edge	0.865	20
Band 9—Water vapor	0.945	60
Band 10—SWIR—Cirrus	1.375	60
Band 11—SWIR1	1.610	20
Band 12—SWIR2	2.190	20

Note: SWIR = short-wave infrared.

which was obtained from GEE. Compared with Landsat mission, a moderate resolution satellite, there are a few advantages to choosing the Sentinel-2 mission. The newest Landsat 7 and 8 cross every point on Earth once every 16 days, whereas Sentinel-2 can create images of the same location at least every five days. Another superiority of Sentinel-2 is its 10 m resolution for blue, green, red and near infrared (NIR) bands, which represents the key information of a satellite image needed for vegetation detection (*23*). Table 1 shows the relevant information on bands, including their wavelength and resolution. Population demographics were downloaded from the U.S. Census (*24*), and roadway data were downloaded from the GIS database of Leon County, Florida (*25*). Both datasets were imported into ArcMap 10.6 as two-dimensional shapefiles. Population data is presented by census blocks in polygon type, which are the smallest geographic units covering the entire city. Roadway data was imported as line features and bounded with blocks (Figure 2*a*). Data on debris caused by Hurricane Michael were provided by the City of Tallahassee authority (Figure 2*b*). Note that the collected debris in this paper refers only to the material deposited by the hurricane. Data was provided in the comma separated value (CSV) format and converted into a shapefile for further use. Each point of debris has its own longitude, latitude and volume that shows where the debris was loaded and how much debris was collected. Wind gust speed refers to average wind speeds in no more than 20 s, whereas average wind speed indicates the average wind speed in a minute or multiple minutes. Wind gust data was provided by StormGEO Company in 3-h intervals from October 7 to October 15 as 10 m resolution TIFF images. A total of 72 geo-referenced images was obtained.

The selection of factors was done based on the observed impact of Hurricane Michael on the communities and infrastructure of the City of Tallahassee. Roadways were critically affected by downed trees and poles because of high wind speeds. In addition, vegetation debris caused by the hurricane affected the whole city drastically. Roadways can also be affected because of flooding and storm surges, but those impacts are outside the scope of this study. In addition, the impact on power lines and the magnitude of power outages is also critical and can be considered in future work. Other factors associated with socioeconomics, such as household income, health, ethnicity and age, can also be considered as part of the proposed model.

Methodology

In this paper, an integrated methodology is proposed that utilizes both GEE and GIS. Figure 3 shows the flowchart for the overall methodology. Steps of the methodology are discussed in more detail in the following subsections.

GEE. This study utilized GEE to host, visualize, and process Sentinel-2 satellite imagery. GEE is a powerful cloud-based platform that allows for world-wide geospatial analysis and brings the massive computational capabilities of Google to help solve a variety of critical social issues. As such, a preprocessing workflow (Figure 3*a*) was implemented that combines image reduction, image composition, cloud removal and calculation of indices. The preprocessing workflow was applied to Sentinel-2 Level-1C top of atmosphere data. The image collection was first filtered by the region of interest, namely the City of Tallahassee. A composite image from before the hurricane was then retrieved from the period between May 1 and September 1, 2018, whereas the

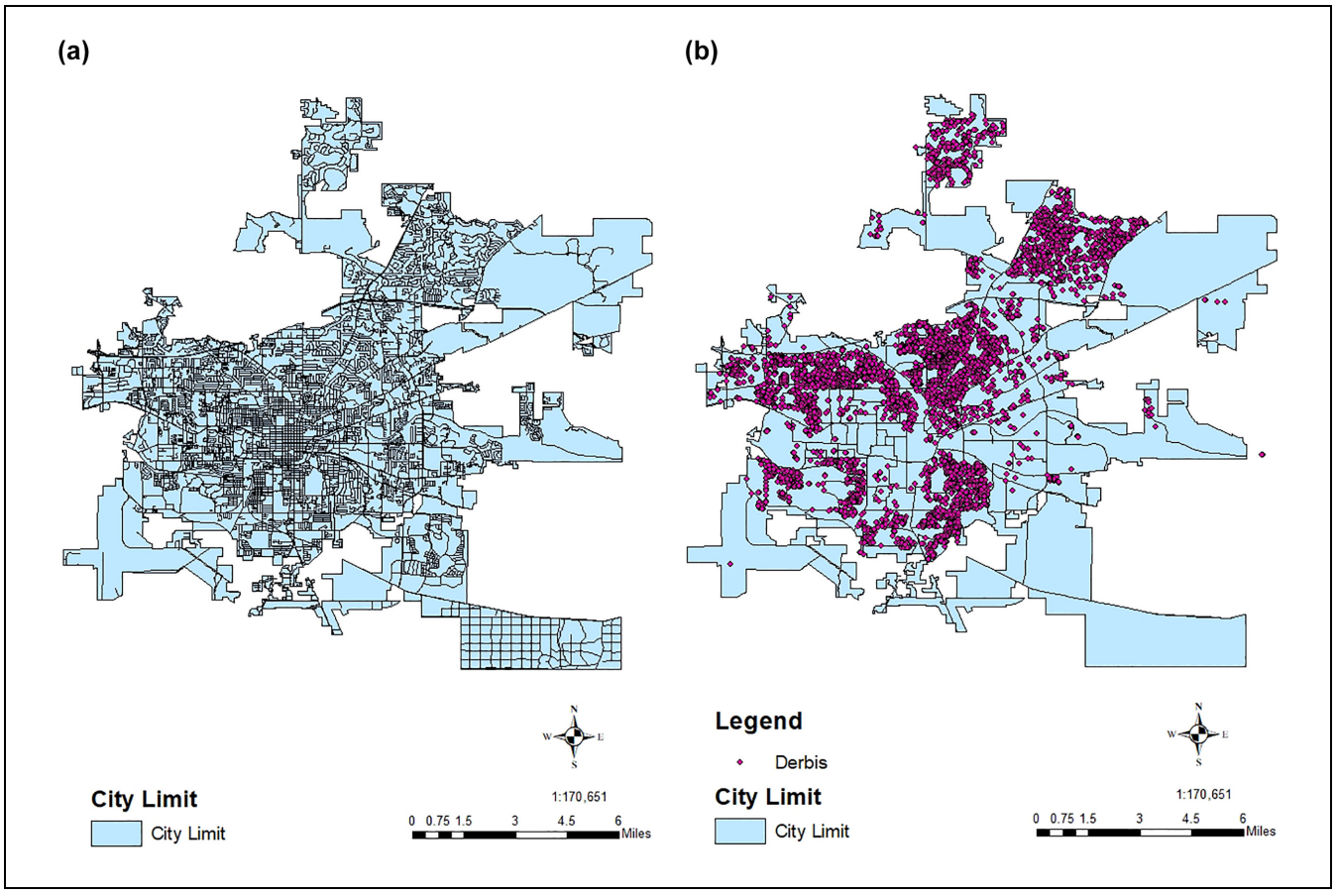

Figure 2. Overview of data: (*a*) roadway network of Tallahassee and (*b*) location of collected debris.

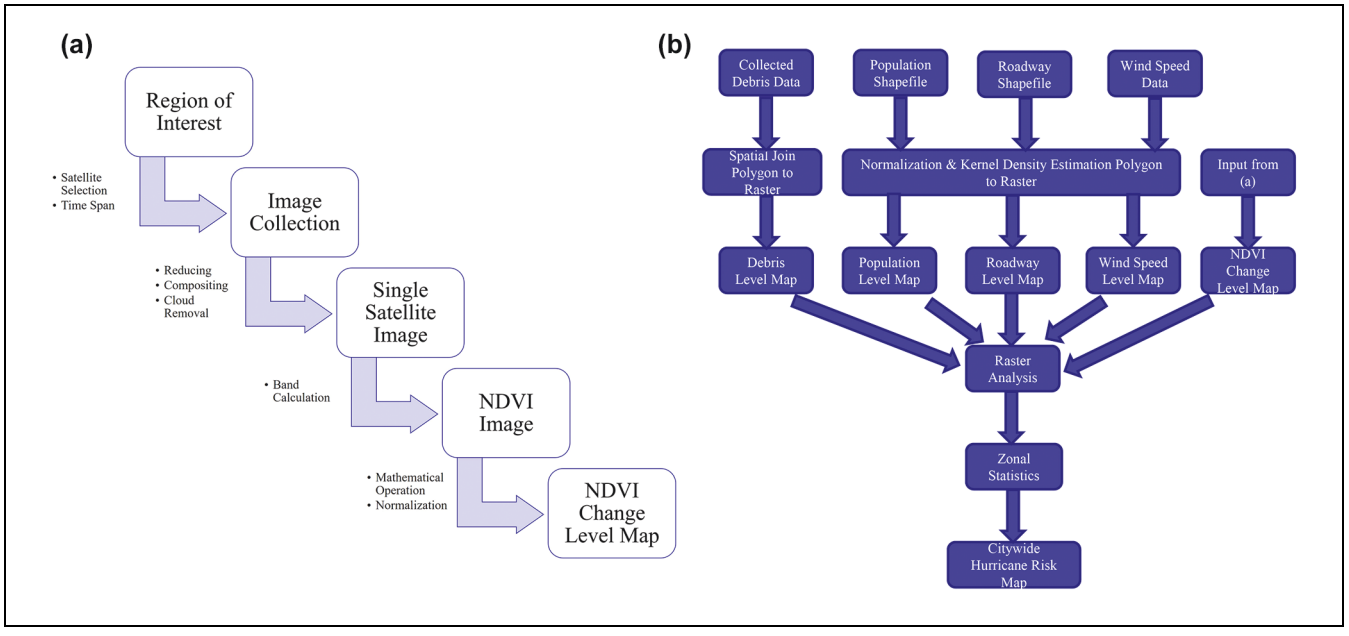

Figure 3. Flowchart for the proposed methodology: (*a*) Google Earth Engine and (*b*) geographical information systems.

after-hurricane image was composited from the period between October 31 and December 31, 2018.

Clouds and cloud shadows have been known to reduce significantly the quality of the image data related to image processing. Therefore, it was imperative to find a way to detect clouds and cloud shadows in the satellite images, and screen them correctly before performing any type of remote sensing activity (*26*). To achieve this, the QA60 bitmask band was employed to cloud mask the image collection. As a result, opaque and cirrus clouds were masked out and images were scaled by 10,000. The collection was also pre-filtered based on its own CLOUDY_PIXEL_PERCENTAGE flag.

To create the best possible picture of the change that happened in Tallahassee because of the hurricane, indices were calculated based on the before and after images, which have the potential to highlight characteristics such as healthy vegetation, bare ground, urban area and others. As the most common vegetation indicator, the NDVI has been succesfully used to analyze green vegetation. Therefore, this paper also utilizes an NDVI-based approach. That is, if vegetation was ripped out by the hurricane, trees would fall down, plants would die and the chlorophyll would greatly decrease, leading to decreased NDVI values. NDVI can be calculated on a per-pixel basis as the normalized difference between the red and near-infrared bands from an image, using Equation 1:

$$\mathrm{NDVI} = \frac{\mathrm{NIR} - \mathrm{RED}}{\mathrm{NIR} + \mathrm{RED}} \tag{1}$$

The vegetation change is defined as the NDVI of the before-hurricane image subtracted from the NDVI of the after-hurricane image based on each pixel. The results were converted and exported to a GeoTIFF image for future analysis in ArcGIS. Note that an NDVI value below 0.2 is often characterized as water, barren areas of rock, sand, or snow. Therefore, the pixels with NDVI value lower than 0.2 were masked out. The average NDVI change was 0.08 per pixel, which indicated that the vegetation of Tallahassee suffered little damage from Hurricane Michael since the hurricane did not hit the city directly. The change of NDVI can also be negative, which indicates an increase in greenness. This may happen since trees may fall on roadways and other places, increasing the NDVI values of those locations but decreasing the NDVI values for their original locations.

GIS. By integrating different types of data on wind speed, debris, roadway density based on the length of roadways and demographics in ArcGIS, impact maps were obtained for the City of Tallahassee. For this purpose, a "Raster Analysis" was conducted to create two normalized weighted impact indices (NWII) for each census population block. The first NWII (NWII_1) is based on the scenario in which all the factors are considered with equal importance. However, the population density of an area can be one of the most important determining factors for developing better emergency-focused plans and policies. As such, understanding how many people live in a particular area can help agencies develop area-specific further improvements such as roadway modification. Thus, the second NWII (NWII_2) represents simply the population density-based weighted average. The estimation of NWII_2 is a multistep process (Figure 3*b*). The definitions of the two impact indices for the proposed methodology are given in Equations 2 and 3, as follows:

$$\mathrm{NWII}_1 = w_1 C_{PB} + w_2 D_{PB} + w_3 W_{PB} + w_4 R_{PB} + w_5 P_{PB} \tag{2}$$

$$\mathrm{NWII}_2 = \frac{\sum_{i=1}^{n}((C_i + D_i + W_i + R_i)^{*}\mathrm{Pop}_i)}{\sum_{i=1}^{n}\mathrm{Pop}_i} \tag{3}$$

where C represents the vegetation change data, D is collected debris data, W is wind speed data, R is the roadway length, P is the population and w values represent the respective weight factors for NWII_1, and i is the pixel number.

Input data of all factors were first summed up in each population block, and the index was calculated on a per-pixel basis. The debris data were first imported to ArcMap and converted into a shapefile. "Spatial Join" tool was used to calculate the debris within each population block. The length of roadways in each population block was also summed up to represent an urban utilization factor. The density distribution of the magnitude of wind speed was determined using a kernel density estimation (KDE)-based approach. A total 72 geo-referenced wind speed images were first merged into a raster with the maximum value of each pixel followed by a zonal analysis to calculate the average wind gust in each population block group.

Next, normalization was performed to find the intensity level of each factor (e.g., wind speed level, debris level, roadway network level). To normalize the input data, a new field was created in each impact factor's attribute table to calculate a normalized value for each factor. This value was then divided into 10 equal intervals and labeled as "1" to "10," where value of 1 indicated the least intensity of factor and a value of 10 indicated the most intensity of factor. Zero values were given a value of zero in the normalized fields. These new intensity classes of each factor were converted from vector to raster using the "Polygon to Raster" tool. Lastly, all the rasterized impact factors were combined into one map based on raster analysis using the aforementioned impact index equations. For NWII_1, the "Weighted

Sum" tool was used, which multiplied each raster by the weight factor and then summed all the values. Since there are just five factors, the weight was equally distributed for $NWII_1$. "Raster Calculator" was the key tool to calculate $NWII_2$ which allows users to perform mathematical operations on each pixel. The weighted impact maps for both indices were created to identify the impact level for the whole city, examine critical locations, and conduct an assessment with respect to roadway disruptions.

Results

Impact Factors

Figure 4 shows an example of pre-processed median Sentinel-2 composites (Figure 4*a*), an NDVI image of before and after Hurricane Michael (Figure 4*b*), an NDVI change map (Figure 4*c*), and converted shapfile of vegetation change per census block (Figure 4*d*). The maximum and minimum NDVI values were found to be 0.853 and –0.441, respectively. It can be observed that the NDVI image from before Hurricane Michael showed darker green than the after image, which indicates that NDVI values have decreased for many areas, especially in the northeast and southwest of Tallahassee. This is because the usually green tropical vegetation had been ripped out by the strong winds of Hurricane Michael. The change map also indicates that most of the city experienced at least a medium to high decrease in the vegetation change.

The debris status was mapped in Figure 5*a*. It can observed that most of the debris was collected diagonally, from the east to the north of the city. Census blocks located in the Lake Bradford area were found to have the largest debris volume of 27,175 cubic yards. The average debris was estimated to be 2,585 cubic yards. The roadway urbanization map is presented in Figure 5*b*. It appears that southeast Tallahassee has the densest roadway network compared with other locations. Central Tallahassee was also found to include many roadways, because of its high roadway density, as well as the northeast section of the city. Figure 5*c* indicates that an area on the west side of Tallahassee experienced higher wind speeds than other locations since Hurricane Michael's path was closer to the west of the city. This led to higher impact levels in the west of Tallahassee. Note that wind speeds ranged between 62 and 76 mph. A different hurricane could have a different path than Hurricane Michael, and different sections of the city would be affected accordingly. Figure 5*d*, on the other hand, demonstrates the demographics based on the population density. The most populated block is in the southeast of Tallahassee, namely Southwood. It also reveals that the northeast side of the city also has a higher population.

NWII

After all the impact factors were estimated, the impact index maps were created using "Zonal Statistics" to calculate average impact levels for each census block. Figure 6 demonstrates both NWIIs for the City of Tallahassee. Visual inspection of Figure 6*a* shows that major portions of Tallahassee appear to experience a moderate impact level based on the integrated data sets, including the weather, debris, demographics, roadways and vegetation. The highest impact locations were found to be the west and north sections of the city. The areas around the Seminole Manor and Mary Manor districts, as well as the Ox Bottom Manor and Summerbrook districts, especially, were found to experience higher risk of hurricane-induced disruptions such as roadway closures. That is, these areas have higher possibility of high wind speeds, debris and vegetation change, and the northeast side of the town has a greater older adult population, which makes the problem even more challenging. The southeast of the city, the Southwood area, has also been found to be affected more than other locations. The proposed weighted index can provide higher values because of high levels of urbanization (represented as the total length of the roadways in a census block), even though the impacts of wind and vegetation because of Michael were not high in these areas.

Figure 6*b*, on the other hand, shows different results based on the population density weighted averages. This type of analysis can be conducted with weighting on other factors as well and this paper simply considered the population only. This map shifts the high impact areas to the central and west sides of Tallahassee since the population is higher in those areas. They include the two universities (Florida State University and Florida A&M University) and one community college (Tallahassee Community College) and are highly populated by government agency personnel since Tallahassee is the state capital. Compared with Figure 6*a*, the Southwood area showed lower impact in Figure 6*b*. The reason is that, even though the population of the Southwood area is high, the density is relatively low because of the large census block area. On the contrary, a small census block with extremely high population density above the Southwood area has been affected more, as seen in Figure 6*b*.

It is absolutely critical to validate the proposed model; however, this requires the availability of data from multiple hurricanes and locations. Given that hurricanes are rare events, this becomes a challenging issue. Nevertheless, in the future, the authors believe they can test and validate the proposed model with data obtained from other recent hurricanes such as Hermine and Irma.

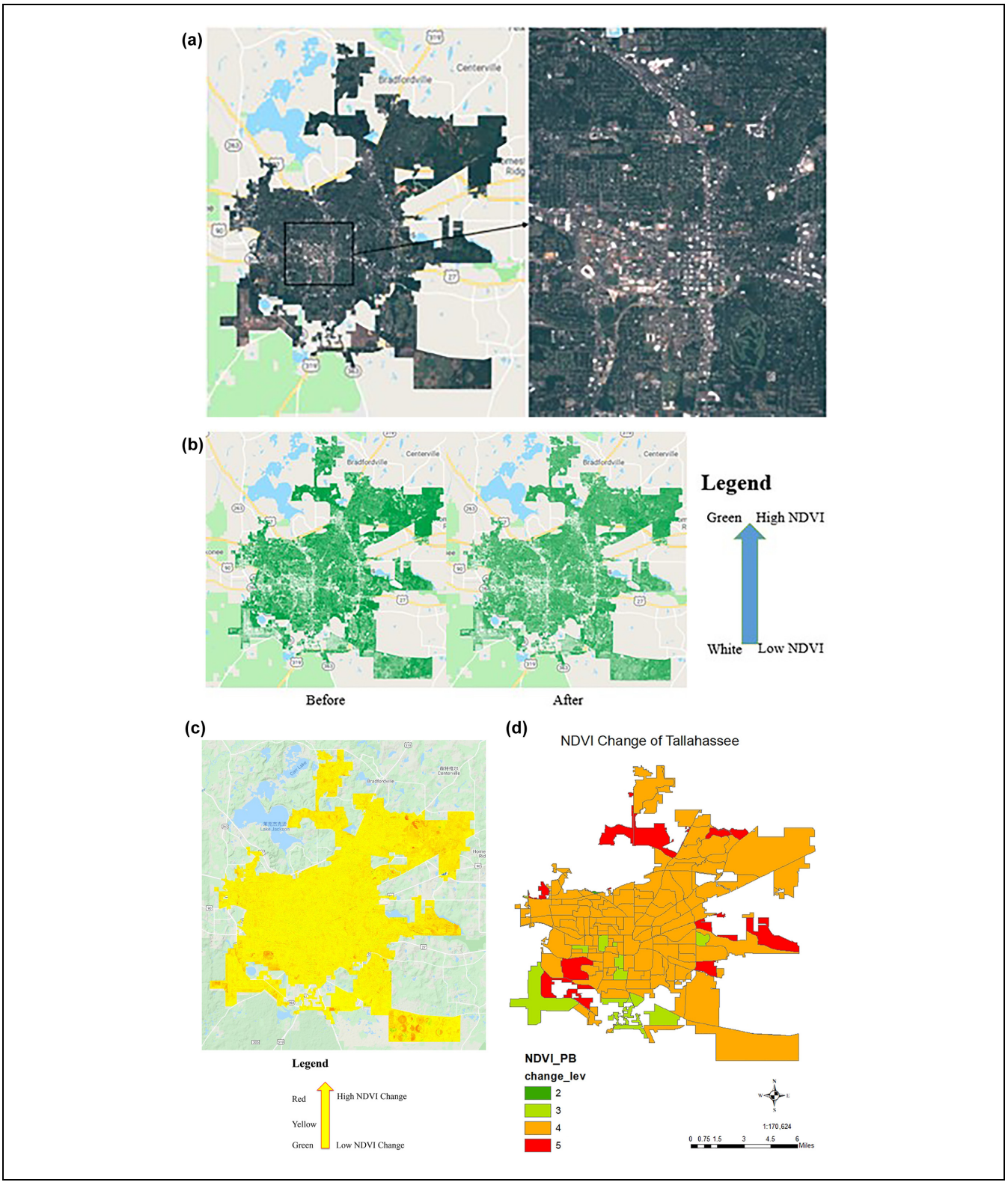

Figure 4. Overview of vegetation change: (*a*) Sentinel-2 satellite image of Tallahassee, (*b*) Normalized Difference Vegetation Index (NDVI) image, (*c*) NDVI change in Google Earth Engine and (*d*) NDVI change in geographical information systems (GIS).

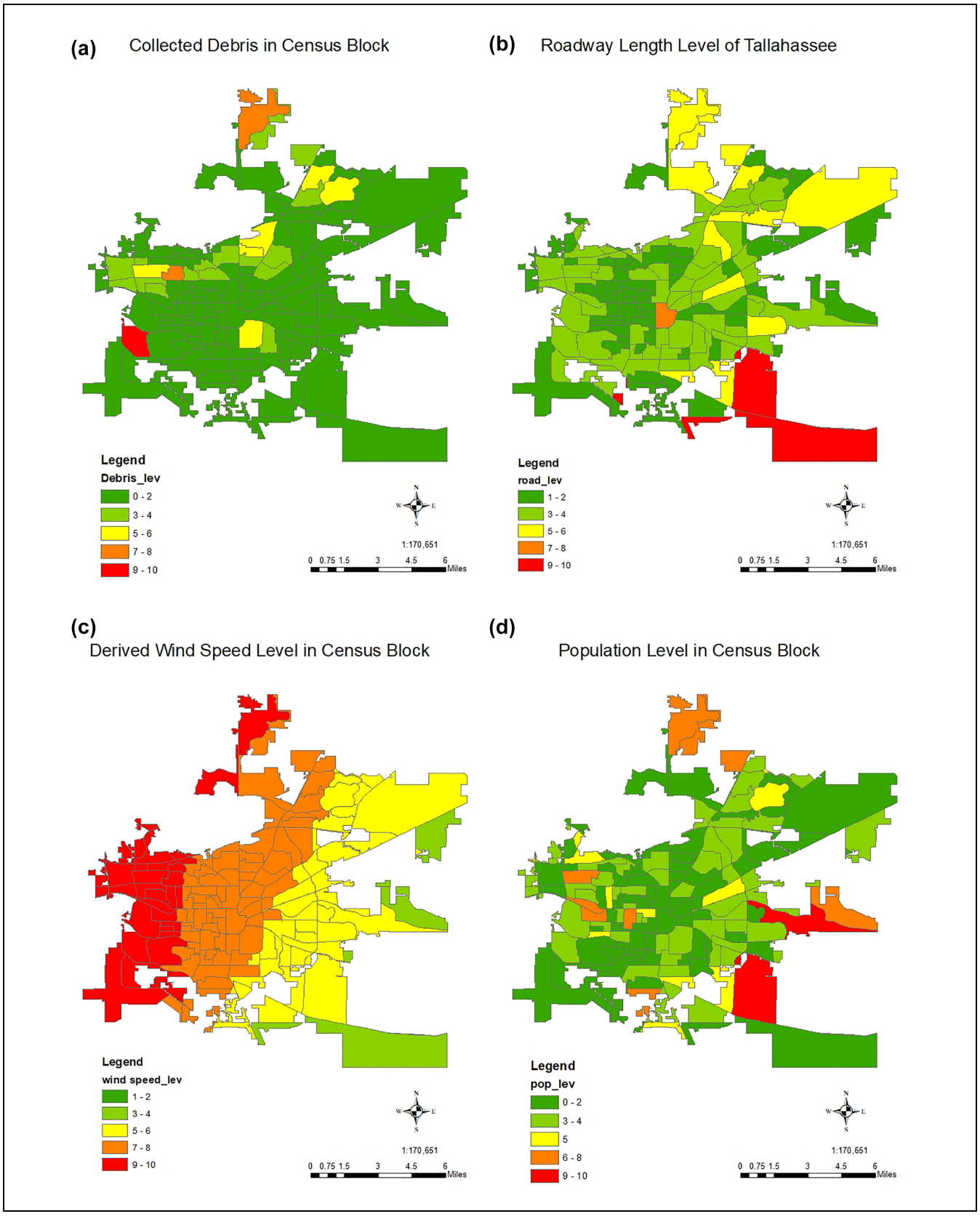

Figure 5. Overview of impact factors mapped by census block: (*a*) debris, (*b*) roadways, (*c*) wind speed and (*d*) population density.

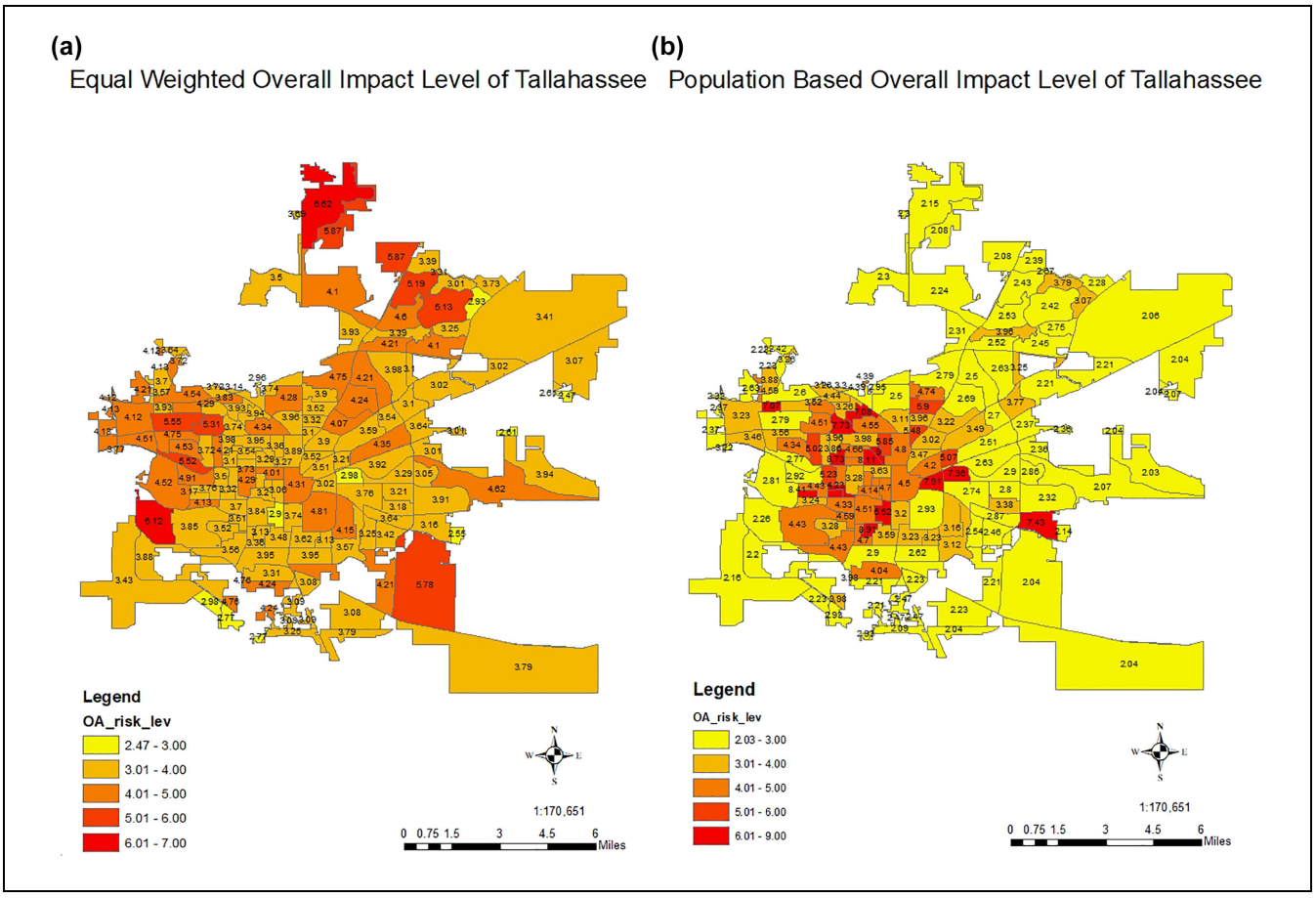

Figure 6. City-wide hurricane impact maps for the City of Tallahassee: (*a*) equally weighted and (*b*) population weighted.

Following the validation, the developed technique can also be utilized for predicting vulnerabilities because of cascade failures (e.g., power outages and roadway closures because of downed trees, roadway closures because of downed power lines or flooding because of storm water as well as the impact of these disruptions on emergency response times), which was experienced in all the recent hurricanes. This would especially be useful to cities when setting priorities in their improvement programs and for regulating vegetation management through zoning, and it is an excellent future work direction.

Conclusions and Future Work

This study presented a two-stage model to analyze the impact of Hurricane Michael on the City of Tallahassee and developed city-wide hurricane impact maps at the level of census blocks. The first stage included a complete preprocessing workflow in GEE, including well-established algorithms of image reduction, image composition, cloud removal and index calculation. The next stage included a GIS-based analysis to create impact maps for the city based on equal weights and population-based weights. The information gained by such an investigation can assist city officials in identifying critical and less resilient regions, and determining those demographic and socioeconomic groups which were more affected by the adverse consequences of the hurricane. For example, findings showed that the northeast side of the city had high impact levels, which is a region where more senior populations (aged 65 and above) live, and disruptions on that side of the city could lead to dramatic consequences because of the fragility of these seniors. City officials can pinpoint the identified critical locations for future improvements such as roadway geometry modification and landscaping justification. Governments might consider having emergency response plans in critical locations for future hurricanes.

This paper extensively discussed why the Sentinel-2 satellite mission was chosen. The newest Landsat 7 and 8 cross every point on Earth once every 16 days, whereas Sentinel-2 can create images of the same location at least every five days. However, an orbital period of five days is still a considerable time interval and this interval may lead to loss of some important information during a hurricane. Future research should pay attention to this

limitation and explore ways to improve it. Due to limited data access, few factors including population, roadway, derbis, vegetation and wind speed were selected to derive the impact index. These factors were drastically affected by the impact of Hurricane Michael. In addition, the impact on power outages or other socioeconomics factors such as housing, education, health, ethnicity and agea is also critical and can be considered as part of the proposed model in future work.

This study focused only on the City of Tallahassee; however, the proposed methodology can be successfully extended to other locations given the availability of data. The proposed impact index could be enhanced using relevant data on rainfall, power grid and power outages, and socioeconomics. The proposed effort mainly focuses on assessing the impact of Hurricane Michael on the City of Tallahassee. Given the availability of data from multiple hurricanes and locations, the developed indices can definitely be utilized for prediction purposes. That is, the developed technique can be utilized for predicting vulnerabilities because of cascade failures (e.g., power outages and roadway closures because of downed trees, roadway closures because of downed power lines or flooding because of storm water as well as the impact of these disruptions on emergency response time), which were experienced in all the recent hurricanes. This predictive analysis can be regularly performed at pre-determined time intervals such as three or five years. This would be especially useful to city authorities when setting priorities in their improvement programs and for regulating vegetation management through zoning, and it is an excellent future work direction. While making such a prediction possible, it is critical to perform sensitivity analyses based on the rate of change of key inputs to guide the adaptive management based on the model. In future work, the proposed model will also be tested with data obtained from other recent hurricanes such as Hermine and Irma. Based on the performance of the model with different input parameters, city governments can perform sensitivity-analysis based risk assessments and make informed emergency management decisions.

Acknowledgment

The authors would like to thank the City of Tallahassee and StormGeo for providing data.

Author Contributions

The authors confirm contribution to the paper as follows: study conception and design: Mingyang Chen, Tarek Abichou and Eren Erman Ozguven; data collection: Mingyang Chen, Alican Karaer, Eren Erman Ozguven, Tarek Abichou and Reza Arghandeh; analysis and interpretation of results: Mingyang Chen, Alican Karaer, Eren Erman Ozguven, Tarek Abichou, Reza Arghandeh and Jaap Nienhius; draft manuscript preparation: Mingyang Chen, Alican Karaer, Eren Erman Ozguven, Tarek Abichou, Reza Arghandeh and Jaap Nienhius. All authors reviewed the results and approved the final version of the manuscript.

Declaration of Conflicting Interests

The author(s) declared no potential conflicts of interest with respect to the research, authorship, and/or publication of this article.

Funding

The author(s) received no financial support for the research, authorship, and/or publication of this article.

References

1. NOAA National Centers for Environmental Information, State of the Climate: Hurricanes and Tropical Storms for Annual 2018, published online January 2019, retrieved on November 3, 2019 from https://www.ncdc.noaa.gov/sotc/tropical-cyclones/201813.
2. National Oceanic and Atmospheric Administration. *Hurricane Michael 2018*. US Department of Commerce, Tallahassee, FL, 2018.
3. Ulak, M. B., A. Kocatepe, L. M. Konila Sriram, E. E. Ozguven, and R. Arghandeh. Assessment of the Hurricane-Induced Power Outages from a Demographic, Socioeconomic, and Transportation Perspective. *Natural Hazards*, Vol. 92, No. 3, 2018, pp. 1489–1508. https://doi.org/10.1007/s11069-018-3260-9.
4. Eskandarpour, R., and A. Khodaei. Machine Learning Based Power Grid Outage Prediction in Response to Extreme Events. *IEEE Transactions on Power Systems*, IEEE, Vol. 32, No. 4, 2017, pp. 3315–3316.
5. Shao, W., M. Gardezi, and S. Xian. Examining the Effects of Objective Hurricane Risks and Community Resilience on Risk Perceptions of Hurricanes at the County Level in the U.S. Gulf Coast: An Innovative Approach. *Annals of the American Association of Geographers*, Vol. 108, No. 5, 2018, pp. 1389–1405. https://doi.org/10.1080/24694452.2018.1426436.
6. Lin, N., J. A. Smith, G. Villarini, T. P. Marchok, and M. L. Baeck. Modeling Extreme Rainfall, Winds, and Surge from Hurricane Isabel (2003). *Weather and Forecasting*, Vol. 25, No. 5, 2010, pp. 1342–1361. https://doi.org/10.1175/2010WAF2222349.1.
7. Kocatepe, A., M. B. Ulak, G. Kakareko, E. E. Ozguven, S. Jung, and R. Arghandeh. Measuring the Accessibility of Critical Facilities in the Presence of Hurricane-Related Roadway Closures and an Approach for Predicting Future Roadway Disruptions. *Natural Hazards*, Vol. 95, No. 3, 2019, pp. 615–635. https://doi.org/10.1007/s11069-018-3507-5.
8. Chang, S. E. Transportation Planning for Disasters: An Accessibility Approach. *Environment and Planning A: Economy and Space*, Vol. 35, No. 6, 2003, pp. 1051–1072. https://doi.org/10.1068/a35195.

9. Li, A. C. Y., L. Nozick, N. Xu, and R. Davidson. Shelter Location and Transportation Planning under Hurricane Conditions. *Transportation Research Part E: Logistics and Transportation Review*, 2012. https://doi.org/10.1016/j.tre.2011.12.004.
10. Wilmot, C. G., and B. Mei. Comparison of Alternative Trip Generation Models for Hurricane Evacuation. *Natural Hazards Review*, Vol. 5, No. 4, 2004, pp. 170–178. https://doi.org/10.1061/(ASCE)1527-6988(2004)5:4(170).
11. Wolshon, B., E. Urbina, C. Wilmot, and M. Levitan. Review of Policies and Practices for Hurricane Evacuation. I: Transportation Planning, Preparedness, and Response. *Natural Hazards Review*, Vol. 6, No. 3, 2005, p. 129. https://doi.org/10.1061/(asce)1527-6988(2005)6:3(129).
12. Ghorbanzadeh, M., M. Koloushani, M. B. Ulak, E. E. Ozguven, and R. A. Jouneghani. Statistical and Spatial Analysis of Hurricane-Induced Roadway Closures and Power Outages. *Energies*, Vol. 13, No. 5, 2020, p. 1098. https://doi.org/10.3390/en13051098.
13. Knorn, J., A. Rabe, V. C. Radeloff, T. Kuemmerle, J. Kozak, and P. Hostert. Land Cover Mapping of Large Areas using Chain Classification of Neighboring Landsat Satellite Images. *Remote Sensing of Environment*, Vol. 113, No. 5, 2009, pp. 957–964. https://doi.org/10.1016/j.rse.2009.01.010.
14. Shalaby, A., and R. Tateishi. Remote Sensing and GIS for Mapping and Monitoring Land Cover and Land-Use Changes in the Northwestern Coastal Zone of Egypt. *Applied Geography*, Vol. 27, No. 1, 2007, pp. 28–41. https://doi.org/10.1016/j.apgeog.2006.09.004.
15. Noi, P. T., and M. Kappas. Comparison of Random Forest, k-Nearest Neighbor, and Support Vector Machine Classifiers for Land Cover Classification using Sentinel-2 Imagery. *Sensors (Switzerland)*, Vol. 18, No. 1, 2018, p. 18. https://doi.org/10.3390/s18010018.
16. Aljoufie, M., M. Zuidgeest, M. Brussel, and M. van Maarseveen. Spatial-Temporal Analysis of Urban Growth and Transportation in Jeddah City, Saudi Arabia. *Cities*, Vol. 31, 2013, pp. 57–68. https://doi.org/10.1016/j.cities.2012.04.008.
17. Van Hell, M. *Detecting Hurricane Induced Changes on Sint Maarten using Sentinel 2 Optical Data. The Effect of Hurricane Irma*. Faculty of Civil Engineering and Geosciences TU Delft, 2018, pp. 1–62.
18. Johansen, K., S. Phinn, and M. Taylor. Mapping Woody Vegetation Clearing in Queensland, Australia from Landsat Imagery using the Google Earth Engine. *Remote Sensing Applications: Society and Environment*, Vol. 1, 2015, pp. 36–49. https://doi.org/10.1016/j.rsase.2015.06.002.
19. Tang, Z., Y. Li, Y. Gu, W. Jiang, Y. Xue, Q. Hu, T. LaGrange, A. Bishop, J. Drahota, and R. Li. Assessing Nebraska Playa Wetland Inundation Status During 1985–2015 using Landsat Data and Google Earth Engine. *Environmental Monitoring and Assessment*, Vol. 188, No. 12, 2016. https://doi.org/10.1007/s10661-016-5664-x.
20. Traganos, D., D. Poursanidis, B. Aggarwal, N. Chrysoulakis, and P. Reinartz. Estimating Satellite-Derived Bathymetry (SDB) with the Google Earth Engine and Sentinel-2. *Remote Sensing*, Vol. 10, No. 6, 2018, p. 859. https://doi.org/10.3390/rs10060859.
21. Lorenzo-Trueba, J., and A. D. Ashton. Rollover, Drowning, and Discontinuous Retreat: Distinct Modes of Barrier Response to Sea-Level Rise Arising from a Simple Morphodynamic Model. *Journal of Geophysical Research: Earth Surface*, Vol. 119, No. 4, 2014, pp. 779–801. https://doi.org/10.1002/2013JF002941.
22. Gorelick, N., M. Hancher, M. Dixon, S. Ilyushchenko, D. Thau, and R. Moore. Google Earth Engine: Planetary-Scale Geospatial Analysis for Everyone. *Remote Sensing of Environment*, Vol. 202, 2017, pp. 18–27. https://doi.org/10.1016/j.rse.2017.06.031.
23. Engels, W.L. Vertebrate Fauna of North Carolina Coastal Islands. A Study in the Dynamics of Animal Distribution I. Ocracoke Island. *American Midland Naturalist*, Vol. 28, No. 2, 2006, p. 273. https://doi.org/10.2307/2420817.
24. United States Census Bureau. Decennial Census Datasets. https://www.census.gov/programs-surveys/decennial-census/data/datasets.2016.html. Accessed April 26, 2019.
25. Street Centerlines - Leon County (LCSTSEG) and GeoData Hub Tallahassee-Leon County GIS. https://geodata-tlcgis.opendata.arcgis.com/datasets/street-centerlines-leon-county-lcstseg. Accessed April 26, 2019.
26. Hu, T., and R. B. Smith. The Impact of Hurricane Maria on the Vegetation of Dominica and Puerto Rico using Multispectral Remote Sensing. *Remote Sensing*, Vol. 10, No. 6, 2018, p. 827. https://doi.org/10.3390/rs10060827.

The contents of this paper and discussion represent the authors' opinions and do not reflect the official views of the City of Tallahassee or of StormGeo.